EURASIP Journal on Applied Signal Processing 2002:6, 601–612

Combined Frequency and Spatial Domain Algorithm for the Removal of Blocking Artifacts

George A. Triantafyllidis
Information Processing Laboratory, Electrical and Computer Engineering Department, Aristotle University of Thessaloniki, Thessaloniki 54006, Greece
Email: gatrian@iti.gr

Dimitrios Tzovaras
Informatics and Telematics Institute, 1st Km Thermi-Panorama Road, Thermi-Thessaloniki 57001, Greece
Email: dimitrios.tzovaras@iti.gr

Demetrios Sampson
Informatics and Telematics Institute, 1st Km Thermi-Panorama Road, Thermi-Thessaloniki 57001, Greece
Email: sampson@iti.gr

Michael G. Strintzis
Information Processing Laboratory, Electrical and Computer Engineering Department, Aristotle University of Thessaloniki, Thessaloniki 54006, Greece

Informatics and Telematics Institute, 1st Km Thermi-Panorama Road, Thermi-Thessaloniki 57001, Greece
Email: strintzi@eng.auth.gr

Received 31 July 2001 and in revised form 7 February 2002

A novel combined frequency and spatial domain method is presented in this paper for blockiness reduction for low bit rate compressed images. The method consists of two stages: in the first, better estimates of the reconstructed DCT coefficients are obtained based on their observed probability distribution. In the second, an efficient postprocessing scheme consisting of a region classification algorithm and a spatial adaptive filtering is applied for blockiness removal. The type of filtering is decided on the basis of an estimation of the local characteristics of the coded image. The main advantage of the proposed method is the efficient combination and design of these two stages which are acting complementarily for the reduction of blocking artifacts. This approach is shown to produce excellent results in removing blocking artifacts. The efficient performance of the proposed algorithm is due, firstly, to the proposition that the shape and the position of the filter kernel are adjusted according to the characteristics of the local image region and secondly, to the employment of the modified improved DCT coefficients by the postprocessing filter. Experimental results illustrating the performance of the proposed method are presented and evaluated.

Keywords and phrases: blocking artifacts, DCT coefficient restoration, spatial adaptive filtering.

1. INTRODUCTION

The block based discrete cosine transform (B-DCT) scheme is a fundamental component of many image and video compression standards. Due to its performance on highly correlated signals which is close to that of the (optimal) Karhunen-Loeve transform (KLT), and the availability of fast software and hardware implementations, the B-DCT is highly popular in application to image compression. In particular, the B-DCT is used in most of current image and video compression standards, such as JPEG [1, 2] and MPEG [3].

A major problem related to the DCT techniques is that the decoded images, especially at low bit rates, exhibit visually annoying gray-level discontinuities along the block boundaries, commonly referred to as blocking artifacts. This is due to the fact that transform coefficient blocks are quantized independently.

Subjective picture quality can be significantly improved by decreasing the blocking artifacts. Increasing the bandwidth or bit rate to obtain better quality images is often not possible or too costly. Several approaches to improve the subjective quality of the degraded images have been proposed in the literature. Techniques which do not require changes to existing standards, appear to offer the most practical solutions, and with the fast increase of available computing power, more sophisticated methods can be implemented.

In the present paper, a new method is presented which acts both in the frequency and the spatial domains, in order to enhance the visual result of the reconstructed image and reduce the blocking artifacts. The proposed algorithm consists of two stages: in the first, better estimates of the AC coefficients are obtained based on observations about their probability distribution. In the second, a region classification is performed, classifying the areas of the image into areas of high detail (textures-edges) and areas of low detail. Then, depending on the classification, a novel efficient adaptive Gaussian-type filtering follows. These two stages are acting complementarily for blockiness removal. In the frequency domain, the modified improved DCT coefficients contributes to blockiness reduction and in the spatial domain, the spatial adaptive filtering furthers the reduction of the blocking artifacts.

In B-DCT the quantization noise is highly correlated with the characteristics of the original signals, so that different areas of the coded image suffer from distinctly different impairments. In particular, the artifacts create two kinds of visual distortions (i) blurring of sharp edges and changes in the texture patterns, and (ii) formation of false edges at interblock boundaries. The first kind of distortion is generally due to near elimination or improper truncation of the high- and mid-frequency DCT coefficients and is efficiently reduced by the proposed AC distribution-based restoration. The other kind is due to severe reductions in the low-frequency DCT coefficients (especially in the DC coefficient) and is tackled with the proposed adaptive spatial filtering. Hence, the two stages are acting complementarily for the removal of blocking artifacts.

Many techniques have been proposed in the literature for the distribution-based estimation of the DCT coefficients. Most of them are based on the fact that there should be a bias in the reconstructed DCT coefficients, since the standard, bin center reconstruction is suboptimal. Particularly, the standard method of restoring a DCT coefficient is equivalent to replacing each coefficient by the center of the quantization interval in which the original coefficient falls. However, the distribution of the AC coefficients for a given frequency peaks at zero and decreases monotonically. Thus, for quantization intervals not including zero, the distribution of the original coefficients is denser at the end of the interval closer to zero making the selection of the center of the interval suboptimal. In this context, the optimal reconstruction (minimum mean squared error) lies in the centroid of the distribution for the interval and such an estimation is employed in this paper.

The novel postprocessing method, described in this paper, exploits the properties of smoothed image gradient data to identify the high- and low-detail regions of the decoded image. The filtering process is then based on the region classification. For the high image detail regions, which include edges and texture, a fully adaptive Gaussian type filter is employed. The shape and the position of the Gaussian kernel is chosen according to the characteristics of each local region. For the low image detail regions, which include areas of constant or slowly varying intensity, a simple Gaussian smoothing operator is used.

The rest of this paper is organized as follows: Section 2 contains a review and discussion of various techniques that have been proposed in the past for the removal of blocking artifacts. In Section 3, the mathematical analysis underlying the concept for the distribution-based restoration of the DCT coefficients is described. Section 4 presents in detail the blocking artifact reduction algorithm by the spatial adaptive filtering procedure. Experimental results, given in Section 5, evaluate visually and quantitatively the performance of the proposed methods. Finally, conclusions are drawn in Section 6.

2. BACKGROUND

Many approaches have been proposed in the literature aiming to alleviate the blocking artifacts in the B-DCT image coding technique. The earliest attempts in enhancing block-encoded images involved space-invariant filtering. Jarske et al. [4] test several filters to conclude that the Gaussian low pass filter with a high pass frequency emphasis gives the best performance. Reeves and Lim [5] apply the 3×3 Gaussian filter only to those pixels along block boundaries. A similar technique by Tzou [6] applies a separable anisotropic Gaussian filter, such that the primary axis of the filter is always perpendicular to the block boundary. It was quickly discovered, however, that space-invariant filters are generally not very effective for this application; they either do not remove enough of the artifacts, or oversmooth the image. Space-varying filters provide a more flexible framework for the reduction of compression artifacts. A space-variant filter that adapts to local characteristics of the signal is proposed by Ramamurthi and Gersho in [7]. The algorithm distinguishes edge pixels from nonedge pixels via a neighborhood testing and then switches between a 1D filter and a 2D filter accordingly to reduce blocking effects. In [8], an adaptive filtering scheme is reported, progressively transforming a median filter within blocks to a low pass filter when it approaches the block boundaries. A region-based method is presented in [9], where the degraded image is segmented by a region growing algorithm, and each region obtained by the segmentation is enhanced separately by a Gaussian low pass filter. Lee et al. in [10] propose a two-dimensional signal adaptive filtering and Chou et al. [11] remove blockiness by performing a simple nonlinear smoothing of pixels. In [12], Apostolopoulos and Jayant propose to identify the blocks that potentially exhibit blockiness by calculating the number of nonzero DCT coefficients in a coded block and comparing it to a threshold. Then, a filter is applied along the boundaries updating the pixels within the distorted block.

Another class of postprocessors using iterative image recovery methods based on the theory of projections onto convex sets (POCS) are proposed in [13, 14, 15]. In the POCS-based method, closed convex constraint sets are first defined that represent all of the available data on the original uncoded image. Then alternating projections onto these convex sets are iteratively computed to recover the original image from the coded image. POCS are effective in eliminating blocking artifacts but less practical for real-time applications, since the iterative procedure adopted increases the computation complexity.

Constrained optimization is the basis of another family of JPEG postprocessors. A subset of this family is known as regularization, a method to solve ill-posed inverse problems. Yang et al. and Zakhor [16, 17] proposed a regularization scheme for a constrained least squares solution, which aims to reconstruct the image by minimizing an objective function reflecting a smoothness property. The constrained least squares approach arises from the desire to remain within the quantization convex set (constraint) but at the same time minimize the highpass energy of the signal (expressed as least squares). Hong et al. [18] also applied regularization methods in the subband domain to reduce DCT artifacts in images.

Another family of postprocessors are based on sophisticated stochastic modeling of the image. All postprocessors use a priori knowledge of the image properties. However, in the model-based approach, the a priori assumptions and their introduction into the algorithm are more explicit. Markov random fields (MRF) are among the more successful models applied to image enhancement. O'Rourke and Stevenson [19] propose a postprocessor that can remove blockiness by maximizing the a posteriori probability (MAP) of the unknown image. The probability function of the decompressed image is modeled by an MRF, and the Huber minimax function is chosen as a potential function. A similar approach is followed by Luo et al. [20]. Li and Kuo [21] developed a multiscale MAP technique, again under the MRF prior. Because of the iterative procedure necessary for the generation of Markov random fields, MRF techniques suffer from high computational complexity.

Among the most simple and effective denoising algorithms are those using the wavelet representation. Gopinath et al. [22] proposed an enhancement method involving the oversampled wavelet transform, in conjunction with a soft thresholding motivated by the minimax arguments of Donoho [23]. Another version of oversampled wavelet denoising was employed by Xiong et al. [24]. Xiong uses an overcomplete wavelet representation to reduce the quantization effects of block-based DCT. Other approaches using wavelet representation are presented in [25, 26]. In [26] the wavelet transform modulus maxima (WTMM) representation is used for image deblocking.

Finally, there are some approaches in the literature which have tackled the problem of blocking artifact reduction completely in the transform domain [27, 28, 29, 30]. In the JPEG standard [1] a method for suppressing the block-to-block discontinuities in smooth areas of the image is introduced. It uses DC values from current and neighboring blocks for interpolating the first few AC coefficients into each block. In [27], Minami and Zakhor present a new approach to reduce the blocking effect, which is applied in the frequency domain. This approach removes the blocking effect by minimizing a new criterion called mean squared difference of slope (MSDS), while imposing linear constraints corresponding to quantization bounds. To minimize the MSDS, a quadratic programming (QP) problem is formulated and solved using a gradient projection method. The solution is obtained in the form of the optimized value of the three lowest DCT coefficients. In [28], Lakhani and Zhong follow the approach proposed in [27] for reducing blocking effects, using however a different solution of the optimization problem, minimizing the MSDS globally and predicting the four lowest DCT coefficients. In [29, 30] a closed form representation of the optimal (in terms of blockiness removal) correction of the DCT coefficients is produced by minimizing a novel enhanced form of MSDS, for every frequency separately. This correction of each DCT coefficient depends on the eight neighboring coefficients in the subband-like representation of the DCT transform and is constrained by the upper and lower bound of the quantized DCT coefficients.

The method proposed in this paper for the reduction of blocking artifacts combines techniques acting in both the frequency and spatial domain. In the DCT domain, new improved and modified DCT coefficients are produced, and in the spatial domain, an adaptive filtering is performed after classification in high- and low-detail areas. The type of filtering is decided on the basis of an estimation of the local characteristics of the coded image. The algorithm of the AC coefficient adjustment is elaborated in the next section while the analysis of the postprocessing spatial filtering is presented in Section 4.

3. DCT COEFFICIENT ADJUSTMENT

In the classical B-DCT formulation, the input image is first divided into 8 × 8 blocks, and the 2D DCT of each block is determined. The 2D DCT can be obtained by performing a 1D DCT on the columns and a 1D DCT on the rows. The 64 DCT coefficients of the spatial block $B_{i,j}$ are then determined by the following formula:

$$F_{ij}(u,v) = \sum_{n=0}^{7}\sum_{m=0}^{7} c_{n,u}c_{m,v}f_{ij}(n,m), \tag{1}$$

where

$$c_{n,u} = a_u \cos\frac{(2n+1)u\pi}{16}, \quad c_{m,v} = a_v \cos\frac{(2m+1)v\pi}{16}, \qquad a_x = \begin{cases} \dfrac{1}{\sqrt{2}} & \text{if } x = 0, \\ 1 & \text{if } x \neq 0, \end{cases} \tag{2}$$

$u, v = 0, \ldots, 7$, $i = 0, \ldots, N/8-1$, $j = 0, \ldots, M/8-1$, $F_{ij}(u,v)$ are the DCT coefficients of the $B_{i,j}$ block, $f_{ij}(n,m)$ is the luminance value of the pixel (n,m) of the $B_{i,j}$ block, and $N \times M$ are the dimensions of the image.

The transformed output from the 2D DCT is ordered so that the DC coefficient $F_{ij}(0,0)$, is in the upper left corner and the higher frequency coefficients follow, depending

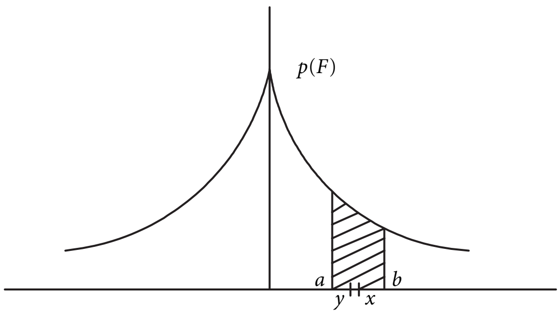

Figure 1: Example of DCT coefficient distribution. The interval (ab) is the quantization interval. The bin center is indicated by the x (i.e., standard reconstruction) and the center of the mass of the distribution over the shaded region is indicated by the y (i.e., optimal reconstruction).

on their distance from the DC coefficient. The higher vertical frequencies are represented by higher row numbers, and higher horizontal frequencies are represented by higher column numbers.

A typical quantization-reconstruction process of the DCT coefficients, as described in JPEG [1], is given by

$$F_{ij}^{Q}(u,v) = \text{round}\left(\frac{F_{ij}(u,v)}{Q(u,v)}\right), \tag{3}$$

$$F_{ij}^{R}(u,v) = F_{ij}^{Q}(u,v)Q(u,v), \tag{4}$$

where $Q(u,v)$ indicates the quantization width bin for the given coefficient, $F_{ij}^{Q}(u,v)$ indicates the bin index in which the coefficient $F_{ij}(u,v)$ falls, and $F_{ij}^{R}(u,v)$ represents the reconstructed quantized coefficient. Then, the reconstructed pixel intensity is obtained from the inverse DCT.

As it has been mentioned in the introduction, B-DCT decoders may be improved by making use of the observation that the distributions of the DCT coefficients peak at zero and decrease algebraically or exponentially with rather heavy tails [31]. An efficient DCT coefficient restoration based on this observation, is made in [32, 33]. Both propose that the unquantized AC coefficients $F_{ij}(u,v)$ are best described by the Laplacian distribution. Considering this distribution of the AC ($i \neq 0$ or $j \neq 0$) coefficients, the standard bin center reconstruction is suboptimal (except for the zero bin). Referring to standard JPEG, any unquantized coefficient $F_{ij}(u,v)$ in the bin denoted by the shaded region (see Figure 1) will be reconstructed to the bin center. However, the minimum MSE is achieved by reconstructing the coefficient to the centroid of the distribution over the given bin.

The Laplacian probability density function (pdf), which models the AC coefficients, is (see [34])

$$f(x) = \frac{a}{2}e^{-a|x|}, \tag{5}$$

and is characterized by the single parameter a. If the Laplacian-modeled variable is quantized using uniform step sizes, the only information available to the receiver is that the original DCT coefficient is in the interval

$$\gamma - t \leq F_{ij}(u,v) \leq \gamma + t, \tag{6}$$

where $\gamma = F_{ij}^{Q}(u,v)Q(u,v)$, $t = Q(u,v)/2$. The trivial solution suggested in JPEG is to reconstruct the coefficient in the center of the interval as $F_{ij}^{R}(u,v) = \gamma$, which simplifies implementation. As mentioned, the optimal reconstruction γ' (minimum mean squared error) lies in the centroid of the distribution for the interval $(\gamma - t, \gamma + t)$, thus, under the assumption of Laplacian statistics [35],

$$\gamma' = \frac{\int_{\gamma-t}^{\gamma+t} x f(x)\,dx}{\int_{\gamma-t}^{\gamma+t} f(x)\,dx} = \gamma + \frac{1}{a} - t\coth(at). \tag{7}$$

Note that this implies a bias δ toward the origin,

$$\delta = \gamma - \gamma' = t\coth(at) - \frac{1}{a}. \tag{8}$$

For different coefficients we have different step size and parameter a [32]. Therefore, considering the DCT coefficient of block $B_{i,j}$ at frequency (u,v), we have quantization step size $Q(u,v)$ and parameter $a_{ij}(u,v)$. Then, the bias δ_{ij}^{uv} toward the origin can be found from (8) and (6):

$$\delta_{ij}^{uv} = \frac{Q(u,v)}{2}\coth\left(\frac{a_{ij}(u,v)Q(u,v)}{2}\right) - \frac{1}{a_{ij}(u,v)}. \tag{9}$$

Thus, we obtain the optimal estimation $\hat{F}_{ij}^{R}(u,v)$ of the reconstructed AC coefficient,

$$\begin{aligned}\hat{F}_{ij}^{R}(u,v) &= F_{ij}^{R}(u,v) - \text{sign}\left[F_{ij}^{Q}(u,v)\right]\delta_{ij}^{uv}\\ &= F_{ij}^{Q}(u,v)Q(u,v) - \text{sign}\left[F_{ij}^{Q}(u,v)\right]\delta_{ij}^{uv},\end{aligned} \tag{10}$$

where the sign function is appropriately used to handle both positive and negative values and $\text{sign}[0] = 0$.

The parameter a, which characterizes the Laplacian distribution and which is needed for the coefficient estimation in (10), can be estimated through two different methods.

In [32], an estimate of a is found by simply computing the variance σ_F^2, of the dequantized coefficients reconstructed to bin center and then setting $a = \sqrt{2}/\sigma_F$, which is a well-known relation between the Laplacian parameter and the variance of the distribution.

Price [33] suggests a more rigorous, ML estimate for the parameter a. Assuming the Laplacian distribution, suppose that we have a series of N observations of a given coefficient $F_{ij}^{R}(u,v)$, prior to any quantization. Referring to these observations as F_k for $k = 1, \ldots, N$, it is easily shown that the ML estimate of a is given by

$$a_{\text{ML}} = \frac{N}{\sum_{k=1}^{N}|F_k|}, \tag{11}$$

where it is assumed that the summation in the denominator does not reduce to zero. The decoder side, however, does not have access to the original, unquantized coefficients. Therefore, the parameter a must be estimated from the reconstructed coefficients. Referring to the quantized coefficients by F_k^Q, and the Laplacian parameter by a_{ML}^Q, it can be shown that (see [33])

$$a_{\mathrm{ML}}^Q = \frac{2}{Q}\ln(\gamma), \tag{12}$$

where

$$\gamma = -\frac{N_0 Q}{2NQ+4S} + \frac{\sqrt{N_0^2 Q^2 - (2N_1 Q - 4S)(2NQ+4S)}}{2NQ+4S} \tag{13}$$

and where N_0 is the number of observations that are zero, N_1 is the number of observations that are not zero, N is the total number of observations ($N = N_0 + N_1$), and $S = \sum_{k=1}^{N} |F_k^Q|$.

Although the Laplacian distribution model remains a popular choice balancing simplicity and fidelity to the empirical data, researchers have tried a variety of other fitting methods for the DCT coefficients, such as χ^2, Kurtosis and Watson tests [36, 37]. Many other possible distribution models have also been proposed including generalized Gaussian and even a sum of Gaussian distributions [37]. Generalized Gaussian densities describe the AC coefficients quite accurately [38], since they have heavy tails [39]. However, these coefficients can be described even more accurately by the α-stable pdf [40], which is a rich and flexible modeling tool. The α-stable density can be best described by its characteristic function, which is

$$\phi(\omega) = e^{j\delta\omega - g|\omega|^{a}[1+j\beta\,\mathrm{sign}(\omega)\phi(\omega,a)]}, \tag{14}$$

where

$$\phi(\omega, a) = \begin{cases} \tan\dfrac{a\pi}{2} & \text{for } a \neq 0, \\ \dfrac{2}{\pi}\log|\omega| & \text{for } a = 1. \end{cases} \tag{15}$$

This density is completely described by the following four parameters: the location parameter δ ($-\infty < \delta < \infty$), the scale parameter g ($g > 0$), the index of skewness β ($-1 \leq \beta \leq 1$), and the characteristic exponent α ($0 < \alpha \leq 2$). The symmetric α-stable SaS family (in which $\beta = 0$) is often used to describe non-Gaussian signals characterized by heavy-tailed distributions, like the low frequency DCT coefficients. The characteristic exponent a determines the shape of the density as it measures the "thickness" of the tails of the density. For smaller values of a the tails of the density are heavier and the corresponding random process displays high impulsiveness. The SaS density with $a = 1$ corresponds to the Cauchy density [40]. Thus, the Cauchy density can be considered as a better distribution model for the AC coefficients, since it is a more heavy-tailed than the Laplacian and the generalized Gaussian densities.

The pdf of the Cauchy model is the following:

$$f(x) = \frac{1}{\pi}\frac{g}{g^2 + (x-\delta)^2}. \tag{16}$$

Recall that the optimal solution for the DCT coefficient is achieved by reconstructing the coefficient to the centroid of the distribution for the interval $\gamma - t, \gamma + t$. Then, we obtain, similarly to (7), the following result based on the assumption of a Cauchy distribution of the AC coefficients:

$$\gamma' = \frac{\int_{\gamma-t}^{\gamma+t} x f(x)\,dx}{\int_{\gamma-t}^{\gamma+t} f(x)\,dx} = \frac{\left[g\ln\left(x^2+g^2\right)\right]_{\gamma-t-\delta}^{\gamma+t-\delta}}{\left[\arctan(x/g)\right]_{\gamma-t-\delta}^{\gamma+t-\delta}} + \delta, \tag{17}$$

where $[f(x)]_l^k = f(k) - f(l)$. The Cauchy parameters g and δ are computed using the ML method.

4. POSTPROCESSING USING SPATIAL ADAPTIVE FILTERING

Following the description of the main picture quality impairments due to low bit rate B-DCT compression scheme and after the biased reconstruction of the DCT coefficients, the design requirements of the proposed efficient postprocessing method can be outlined as follows. The compressed image is initially segmented into different regions, which correspond to areas that suffer from different types of degradation. Hence, a classifier, which distinguishes the smooth regions from the detailed ones, needs to be employed.

Provided that the above step has been implemented successfully, an adaptive filtering technique takes into consideration the characteristics of the quantization noise in different areas of the coded image. More specifically:

- staircase noise along the edges must be removed, so that edges appear continuous and sharp. This requires smoothing along, but not across, the edge direction to avoid blurring;
- false contours visible in the areas of slowly-varying intensity should be eliminated. This requires smoothing of the intensity changes that occur between adjacent blocks;
- the disturbing blocking effect should also be removed from textured areas, while any high-detail that survived during the coding process should be preserved.

The proposed method employs a useful tool in the description of local image features, known as windowed second moment matrix (WSMM) [41], whose elements are the locally-smoothed functions of the image derivatives. Information provided by the WSMM has been utilized for a number of computer vision tasks, such as the detection of feature points and the extraction of shape information from texture areas [41].

Let $P(x, y)$ denote the image intensity value at point (x, y). The image gradient $\nabla P = (G_x, G_y)^T$ is computed as follows:

$$\begin{aligned} G_x(x, y) &= \frac{P(x+1, y) - P(x-1, y)}{2}, \\ G_y(x, y) &= \frac{P(x, y+1) - P(x, y-1)}{2}. \end{aligned} \tag{18}$$

The WSMM is then defined as (see [42])

$$W = \begin{bmatrix} A & C \\ C & B \end{bmatrix}, \tag{19}$$

$$\begin{aligned} A &= \sum_{(x,y)\in(M\times M)} w_b(x,y) G_x^2(x,y), \\ B &= \sum_{(x,y)\in(M\times M)} w_b(x,y) G_y^2(x,y), \\ C &= \sum_{(x,y)\in(M\times M)} w_b(x,y) G_x(x,y) G_y(x,y), \end{aligned} \tag{20}$$

where $M\times M$ is the analysis block, that is, the area from where information is obtained for the calculation of the WSMM components A, B, and C. The function $w_b(x, y)$ is a symmetric and normalized window function which is used for local smoothing of the image features. This is necessary due to the sensitivity of the first order derivatives of image intensity to noise. A natural choice for $w_b(x, y)$ is a Gaussian function of the form $w_b(x, y) = e^{-(x^2+y^2)/2\tau^2}$.

The WSMM coefficients are then employed to perform the tasks required for the removal of annoying artifacts from the compressed images, namely, region classification and filtering.

4.1. Region classification

A simple algorithm based on the values of the WSMM coefficients is used to distinguish low-detail areas from the high-detail ones in the coded image. The quantities A and B, defined in (19), contain information about the local edge strength [41, 43]. It is expected that a large value of either of them will be due to the presence of a jagged edge or image texture. This is especially true when the area of smoothing defined by parameter M is chosen to have size similar to the coding block. Thus, region classification is performed by comparing the values of A and B against a predetermined threshold T [43]. If at least one of them exceeds T then the corresponding picture element is assumed to belong to a high-detail area of the image; otherwise, it is assumed to lie in a uniform low-detail area. The filtering strategy is then decided according to the outcome of the classification.

4.2. Filtering

4.2.1 Filtering of high-detail areas

The purpose of the postprocessing in high-detail areas is twofold: to eliminate the visible noise from the edges and to preserve any detail that remains in the texture blocks. A new adaptive filtering operation which satisfies both requirements is employed in this paper. The process computes for a pixel a Gaussian-type kernel, which is shaped and displaced according to locally smoothed image gradient functions [44]. The filter kernel $K(x, y)$ is then defined as follows:

$$K(x,y) = \frac{1}{S} e^{-(\hat{A}(x+D_x)^2 + 2\hat{C}(x+D_x)(y+D_y) + \hat{B}(y+D_y)^2)/2\sigma^2}, \tag{21}$$

where S is a normalization factor defined [43] as

$$S = \sum_{(u,v)\in(N\times N)} e^{-(\hat{A}(u+D_u)^2 + 2\hat{C}(u+D_u)(v+D_v) + \hat{B}(v+D_v)^2)/2\sigma^2}, \tag{22}$$

and N is the side length of the square truncation mask that contains the kernel, σ is the standard deviation of the variable Gaussian kernel, $\hat{A}$, $\hat{B}$, and $\hat{C}$ are the coefficients of the WSMM normalized by division by $A + B$ to reduce image dependency problems [44], and D_x, D_y determine the magnitude of the kernel displacement along each of the principal axes and are defined as follows [45]:

$$\begin{aligned} D_x &= \frac{N}{2} \frac{V_x}{\sqrt{\mu^2 + V_x^2 + V_y^2}}, \\ D_y &= \frac{N}{2} \frac{V_y}{\sqrt{\mu^2 + V_x^2 + V_y^2}}, \end{aligned} \tag{23}$$

where μ is an attenuation constant and

$$\begin{aligned} V_x &= \frac{1}{A+B} \\ &\quad \times \sum_{(x,y)\in(M\times M)} w_b(x,y) \left[G_x^2(x,y)x + G_x(x,y)G_y(x,y)y \right], \\ V_y &= \frac{1}{A+B} \\ &\quad \times \sum_{(x,y)\in(MM)} w_b(x,y) \left[G_y^2(x,y)y + G_x(x,y)G_y(x,y)x \right]. \end{aligned} \tag{24}$$

The three terms in the exponent adapt the shape of the kernel in such a way that its longest axis is parallel to the edge direction locally dominant in the image [45]. The function of the displacement components, which are also obtained from gradient calculations, is to displace the main weights of the kernel away from edges. The effect is that, when the centre is close to an intensity edge, the main contribution to the convolution comes from the region the centre is in, not from the other side of the boundary, and hence the sharpness of the edge is preserved.

This filter satisfies all the requirements for processing detailed areas of the reconstructed image. First, near an intensity edge the filter kernel is oriented along the edge, which is important in order to avoid blurring. Secondly, the fact that the main weights of the kernel are displaced in or out of the edge (depending on the relative position of the point which is filtered) ensures the continuity and the sharpness of the edge. Finally, the presence of strong intensity discontinuities in different directions has the effect of a reduction in weights away from the centre of the filter kernel, which means that the image details are preserved in textured areas.

4.2.2 Filtering of low-detail areas

For the areas of the image with low detail, the adaptive filter described above is not appropriate. This is due to the fact that intensity changes in the boundaries of neighbouring blocks will be perceived wrongly as corresponding to intensity discontinuities. For these areas simple small-scale Gaussian filtering can smooth the boundaries between coding blocks as required, without introducing any noticeable defects in the output image.

5. EXPERIMENTAL RESULTS

Experiments were carried out to evaluate the performance of the proposed method. In order to show its robustness, a number of known standard 256 gray-level test images were encoded with the block discrete cosine transform-based (DCT-based) JPEG compression algorithm, and then restored using the AC coefficient restoration algorithms presented in Section 3 and the postprocessing spatial adaptive filtering presented in Section 4.

The most appropriate type of distortion measure is based on human perception. The human observer is the end user of most image information. Therefore, a distortion measure that is based on human perception is more appropriate for picture quality evaluation. This type of distortion measure gives a numeric value that will quantify the dissatisfaction of the viewer in observing the reproduced image in place of the original. One method for finding such a measure is subjective testing. In these tests, subjects view a series of reproduced images and rate them based on the visibility of artifacts. Subjective tests are tedious and time-consuming, and the results depend on various other factors such as the observer's background, sensitivity, and so forth.

Therefore, an objective measure that accurately predicts the subjective rating would be a useful guide when optimizing image compression algorithms. There have been several attempts in the past to derive visual models to predict picture quality by means of such objective measures. Most of these models use visual criteria such as the frequency sensitivity and frequency masking properties of the eye.

Such a measure of blocking artifacts is used in this paper in order to evaluate the reduction of the blocking artifacts. Specifically, the HVS-based measure of blocking artifacts is adopted, originally presented in [46]. In [46], Bovik and Liu prove that this metric is very efficient and stable for the blind measurement of blocking artifacts in DCT-coded images. According to this metric, brightness (luminance) masking and activity (texture) masking are the two most significant effects when evaluating the visual perception of blocking artifacts. Masking also depends on the relative orientation [47]. In the following, the blockiness measure of [46] is outlined.

Consider two vertically adjacent 8×8 blocks x_1, x_2. An overlap block is formed composed of the bottom half of x_1, and the top half of x_2 to constitute a new 8×8 block x. A 2D step function in the block x is then defined as follows:

$$u = \begin{cases} -\dfrac{1}{2} & \text{top half of the block } x, \\ \dfrac{1}{2} & \text{bottom half of the block } x. \end{cases} \tag{25}$$

We also define $S = \bar{a} - \bar{b}$ where $\bar{a}$ is the average value of the bottom four rows of x_1, and $\bar{b}$ is the average value of the top four rows of x_2. Since blocking artifacts have two particular directions in the image, vertical and horizontal, an edge distortion will be more masked if the activity in the background has the same orientation. To account for this property, two distinct oriented activities are defined, vertical activity A_v and horizontal activity A_h, as follows:

$$A_v = \sum_{v=1}^{7} v \sum_{u=0}^{7} \left|F(u,v)\right|, \qquad A_h = \sum_{u=1}^{7} u \sum_{v=0}^{7} \left|F(u,v)\right|, \tag{26}$$

where $F(u,v)$ are the DCT coefficients of the overlapped block x [47].

For vertical blocking artifacts (vertically adjacent blocks), the vertical activity will be dominant, hence

$$A_v^{\text{total}} = A_v + qA_h. \tag{27}$$

Similarly, for the horizontal artifacts (horizontally adjacent blocks), the activity may be written as

$$A_h^{\text{total}} = A_h + qA_v, \tag{28}$$

where $q = 0.8$ according to [47].

The masking of artifacts due to activity should vary as a decreasing function of the local activity. Although some more accurate yet complicated models have been advanced [47, 48], in [46] a simple model is proposed to facilitate some real-time applications:

$$S_a = \frac{|S|}{1 + A^{\text{total}}}, \tag{29}$$

where $|S|$ is the amplitude of 2D step function in block x, S_a is the visibility of the artifact after activity masking, and A^{total} can be either A_v^{total} or A_h^{total}, depending on the direction of the blocking artifact being considered (in our case it is A_v^{total}, since we considered the vertically adjacent blocks x_1, x_2). The visibility of the blocking artifact also depends on the brightness of the local background [47, 48]. To account for this phenomenon, we adopt the model proposed in [48], which is

$$S_b = \frac{S_a}{1 + \left(B/B_0\right)^r}, \tag{30}$$

where B is the average value of block x, $B_0 = 150$, and $r = 2$ [46].

These values may be combined to give a numerical metric of the image quality regarding the vertical blocking effect, as follows:

$$S_t = \left(\frac{\sum_{k=1}^{N} \left(S_b\right)_k^p}{N} \right)^{1/p}, \tag{31}$$

where N is the total number of interblock boundaries in the image, S_t is the global measure of the blocking artifacts in the image, and the usual value of the exponent is $p = 4$ [47].

A similar formula for S_t can be produced if we apply the above procedure to the horizontally adjacent blocks. Therefore, since blocking effects in the horizontal and vertical directions generally have no difference in principle, we evaluate the overall image quality metric as the average of the values of S_t metric for the horizontal and vertical directions.

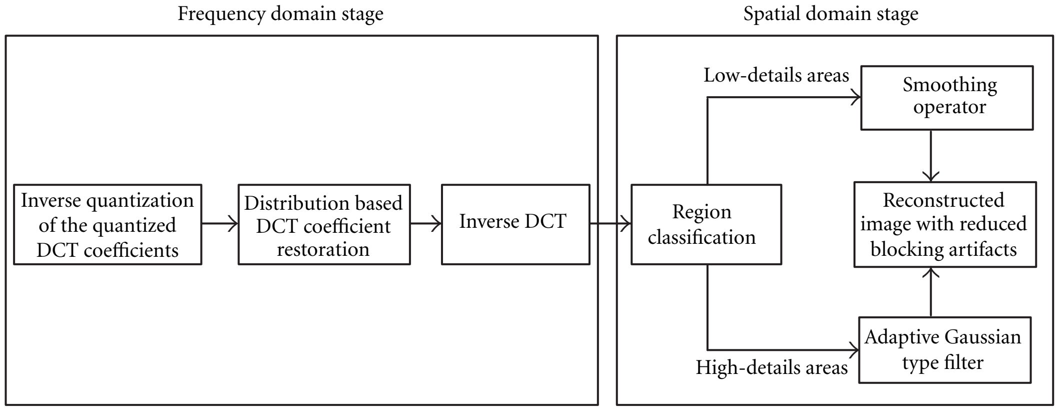

Figure 2: A flow graph of the proposed scheme for blockiness reduction.

Table 1: Blocking artifact measurement in terms of S_t (as defined in [46]) comparing among the standard JPEG compression, the adaptive POCS method of [13], the postprocessing method proposed in [10], our algorithm A (which uses the Laplacian distribution), and our algorithm B (which uses the Cauchy distribution).

Original image	Bit per pixel	JPEG	Algorithm in [13]	Algorithm in [10]	Our algorithm A	Our algorithm B
Lena	0.3 bpp	5.9	5.9	5.7	5.2	5.1
512 × 512	0.4 bpp	3.1	3.0	2.8	2.6	2.6
Peppers	0.3 bpp	6.1	6.0	5.5	5.4	5.4
512 × 512	0.4 bpp	3.3	3.1	2.9	2.8	2.7
Tower	0.3 bpp	2.2	2.1	2.1	2.0	1.9
512 × 512	0.4 bpp	1.3	1.3	1.3	1.1	1.0
Barbara	0.3 bpp	7.9	7.7	7.4	7.1	7.1
512 × 512	0.4 bpp	6.0	5.8	5.8	5.6	5.5
Cameraman	0.3 bpp	7.4	7.4	7.3	7.0	6.9
256 × 256	0.4 bpp	2.9	2.7	2.7	2.2	2.2

In our experiments, the encoded images were decoded using the standard JPEG bin center reconstruction as well as biased reconstruction, as described in Section 3. For biased reconstruction, the three algorithms presented in Section 4 were tested. The first algorithm [32] assumes Laplacian pdf and employs the estimate $a = \sqrt{2}/\sigma_F$, which uses the variances of the reconstructed DCT coefficients, when the second algorithm [33] employs an ML estimation of the Laplacian parameter. Finally, the last algorithm assumes a Cauchy pdf for the AC coefficients.

Experiments show that the best results among these algorithms assuming Laplacian pdf are obtained from the technique [33] which uses the ML estimation of the a parameter, since this seems to be a more efficient estimation of the Laplacian parameter compared to the simple estimation, $a = \sqrt{2}/\sigma_F$. The results obtained under the assumption that the AC coefficients follow a Cauchy distribution are also very promising.

Figure 2 shows the proposed two-fold scheme which was used for our experiments. We compared our method using the metric S_t described above. Table 1 shows the results obtained if S_t is calculated for various images at different bit rates. We compared our algorithm to the method of adaptive POCS in [13] and to the method of [10]. The latter also employs a signal adaptive filtering. Our approach, using either Laplacian distribution or Cauchy distribution, shows a significant reduction of S_t and clearly outperforms the methods in [10, 13] (see Table 1). Comparing the results after applying our algorithm, we infer that results based on the assumption of a Cauchy distribution are better (approximately 3%–10% better) than those based on the assumption of a Laplacian distribution, which was expected, since the Cauchy pdf is a better model for the AC coefficients of the DCT transform. Hence, in our experiments we chose to use the Cauchy pdf coefficient estimation algorithm before applying spatial adaptive filtering.

In Figure 3, the performance of the proposed method for the JPEG compressed Lena image is illustrated. To better investigate the performance of the proposed algorithm, two areas of the image with different characteristics were zoomed in: Figure 4 illustrates a magnified part of the facial area of Lena from the JPEG-coded and the processed image,

(a) (b)

Figure 3: (a) The JPEG coded Lena image at 0.28 bpp. (b) The Lena image after applying the proposed method for blockiness reduction.

(a) (b)

Figure 4: (a) A low-texture portion of JPEG coded Lena image at 0.32 bpp. (b) The same portion of the Lena image after applying the proposed method for blockiness reduction.

(a) (b)

Figure 5: (a) A high-texture portion of JPEG coded Lena image at 0.32 bpp. (b) The same portion of the Lena image after applying the proposed method for blockiness reduction.

(a) (b)

Figure 6: (a) A portion of JPEG coded Barbara image at 0.43 bpp. (b) The same portion of the Barbara image after applying the proposed method for blockiness reduction.

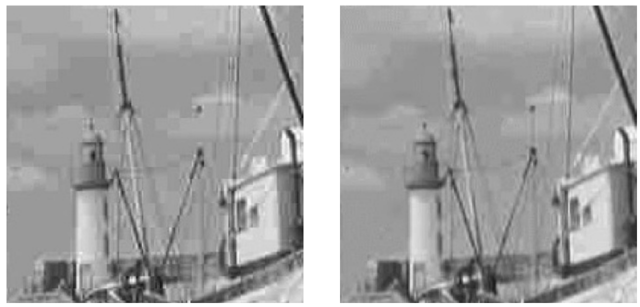

(a) (b)

Figure 7: (a) A portion of JPEG coded Boat image at 0.40 bpp. (b) The same portion of the Boat image after applying the proposed method for blockiness reduction.

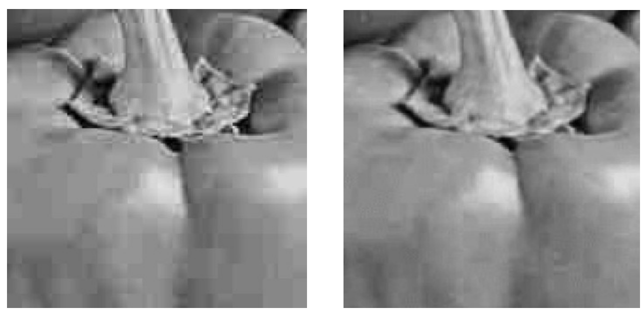

(a) (b)

Figure 8: (a) A portion of JPEG coded Peppers image at 0.35 bpp. (b) The same portion of the Peppers image after applying the proposed method from blockiness reduction.

respectively. It can be seen that blockiness has been reduced in the slowly changing areas of the face. In Figure 5, a part near the hat in the Lena image is magnified. This example illustrates that the noise has been reduced in the edges.

Finally, a visual illustration of the performance of our method, showing the JPEG reconstructed magnified portions of Barbara, Boat, Peppers, Crowd, Tower, and Cameraman images and the corresponding reconstructed portions of the images processed by the proposed method are shown in Figures 6, 7, 8, 9, 10, and 11.

(a) (b)

Figure 9: (a) A portion of JPEG coded Crowd image at 0.45 bpp. (b) The same portion of the Crowd image after applying the proposed method from blockiness reduction.

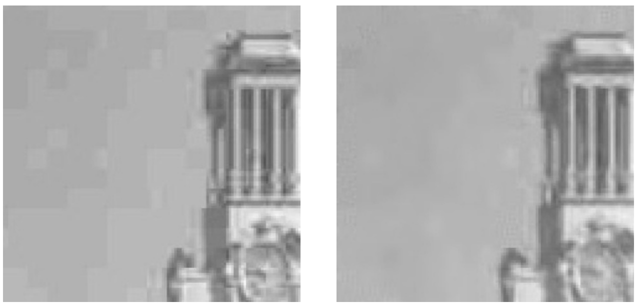

(a) (b)

Figure 10: (a) A portion of JPEG coded Tower image at 0.31 bpp. (b) The same portion of the Tower image after applying the proposed method from blockiness reduction.

6. CONCLUSIONS

When images are compressed using B-DCT transforms, the decompressed images often contain bothersome blocking artifacts which constitute a serious bottleneck for many important visual communication applications. This paper presented a novel algorithm applied in both compressed and spatial domains, in order to reduce these blocking artifacts. In our approach, the Cauchy statistical model is adopted for the AC coefficients and a satisfactory estimation of the DCT reconstructed coefficients is produced. Then, a novel postprocessing procedure consisting of high- and low-detail regions classification and a spatial adaptive filtering is applied for the removal of blocking artifacts. The type of filtering is decided based on an estimation of the local characteristics of the coded image. Experimental results show that the spatial adaptive filter along with the distribution based DCT coefficient restoration is efficient in reducing the annoying blocking artifacts in B-DCT compressed images. In conclusion, the proposed processing algorithm is effective and stable across different images for the reduction of the blocking effects, and thus, enhances JPEG images without the need for any bit rate increase.

(a) (b)

Figure 11: (a) A portion of JPEG coded Cameraman image at 0.51 bpp. (b) The same portion of the Cameraman image after applying the proposed method from blockiness reduction.

REFERENCES

[1] W. B. Pennebaker and J. L. Mitchel, *JPEG Still Image Data Compression Standard*, Van Nostrand Reinhold, New York, NY, USA, 1993.

[2] G. K. Wallace, "The JPEG still picture compression standard," *Communications of the ACM*, vol. 34, no. 4, pp. 30–44, 1991.

[3] K. R. Rao and J. J. Hwang, *Techniques and Standards for Image, Video, and Audio Coding*, Prentice-Hall, Upper Saddle River, NJ, USA, 1996.

[4] T. Jarske, P. Haavisto, and I. Defee, "Post-filtering methods for reducing blocking effects from coded images," *IEEE Trans. Consumer Electronics*, vol. 40, no. 3, pp. 521–526, 1994.

[5] H. C. Reeve and J. S. Lim, "Reduction of blocking artifacts in image coding," *Opt. Eng.*, vol. 23, no. 1, pp. 34–37, 1984.

[6] K. H. Tzou, "Post-filtering of transform-coded images," in *Proc. SPIE Applications of Digital Image Processing XI*, San Diego, Calif, USA, August 1988.

[7] B. Ramamurthi and A. Gersho, "Nonlinear space-variant postprocessing of block coded images," *IEEE Trans. Acoustics, Speech, and Signal Processing*, vol. 34, no. 5, pp. 1258–1268, 1986.

[8] Y.-F. Hsu and Y.-C. Chen, "A new adaptive separable median filter for removing blocking effects," *IEEE Trans. Consumer Electronics*, vol. 39, no. 3, pp. 510–513, 1993.

[9] T. Meier, K. N. Ngan, and G. Crebbin, "A region-based algorithm for enhancement of images degraded by blocking effects," in *Proc. IEEE Tencon '96*, vol. 1, pp. 405–408, Perth, Australia, November 1996.

[10] Y. L. Lee, H. C. Kim, and H. W. Park, "Blocking effect reduction of JPEG images by signal adaptive filtering," *IEEE Trans. Image Processing*, vol. 7, no. 2, pp. 229–234, 1998.

[11] J. Chou, M. Crouse, and K. Ramchadran, "A simple algorithm for removing blocking artifacts in block transform coded images," *IEEE Signal Processing Letters*, vol. 5, no. 2, pp. 33–35, 1998.

[12] J. G. Apostolopoulos and N. S. Jayant, "Postprocessing for low bit-rate video compression," *IEEE Trans. Image Processing*, vol. 8, no. 8, pp. 1125–1129, 1999.

[13] Y. Yang, N. P. Galatsanos, and A. K. Katsaggelos, "Projection-based spatially adaptive reconstruction of block-transform compressed images," *IEEE Trans. Image Processing*, vol. 4, no. 7, pp. 896–908, 1995.

[14] H. Paek, R.-C. Kim, and S.-U. Lee, "On the POCS-based postprocessing technique to reduce the blocking artifacts in transform coded images," *IEEE Trans. Circuits and Systems for Video Technology*, vol. 8, no. 3, pp. 358–367, 1998.

[15] H. Paek, R.-C. Kim, and S.-U. Lee, "A DCT-based spatially adaptive postprocessing technique to reduce the blocking artifacts in transform coded images," *IEEE Trans. Circuits and Systems for Video Technology*, vol. 10, no. 1, pp. 36–41, 2000.

[16] Y. Yang, N. P. Galatsanos, and A. K. Katsaggelos, "Regularized reconstruction to reduce blocking artifacts of block discrete cosine transform compressed images," *IEEE Trans. Circuits and Systems for Video Technology*, vol. 3, no. 6, pp. 421–423, 1993.

[17] A. Zakhor, "Iterative procedures for reduction of blocking effects in transform image coding," *IEEE Trans. Circuits and Systems for Video Technology*, vol. 2, no. 1, pp. 91–95, 1992.

[18] S.-W. Hong, Y.-H. Chan, and W.-C. Siu, "Subband adaptive regularization method for removing blocking effect," in *Proc. 1995 IEEE International Conference on Image Processing*, vol. II, pp. 523 –526, Washington, DC, USA, October 1995.

[19] T. P. O'Rourke and R. L. Stevenson, "Improved image decompression for reduced transform coding artifacts," *IEEE Trans. Circuits and Systems for Video Technology*, vol. 5, no. 6, pp. 490–499, 1995.

[20] J. Luo, C. W. Chen, K. J. Parker, and T. S. Huang, "Artifact reduction in low bit rate DCT-based image compression," *IEEE Trans. Image Processing*, vol. 5, no. 9, pp. 1363–1368, 1996.

[21] J. Li and C.-C. J. Kuo, "Coding artifact removal with multiscale postprocessing," in *Proc. 1997 IEEE International Conference on Image Processing*, vol. 2, pp. 529–532, Santa Barbara, Calif, USA, October 1997.

[22] R. A. Gopinath, M. Lang, H. Guo, and J. E. Odegard, "Wavelet-based postprocessing of low bit rate transform coded images," in *Proc. 1994 IEEE International Conference on Image Processing*, vol. 2, pp. 913–917, Austin, Tex, USA, 1994.

[23] D. Donoho, "Denoising by soft thresholding," *IEEE Transactions on Information Theory*, vol. 41, no. 3, pp. 613–627, 1995.

[24] Z. Xiong, M. T. Orchard, and Y. Q. Zhang, "A deblocking algorithm for JPEG compressed images using overcomplete wavelet representations," *IEEE Trans. Circuits and Systems for Video Technology*, vol. 7, no. 2, pp. 433–437, 1999.

[25] R. Molina, A. K. Katsaggelos, and J. Abad, "Bayesian image restoration using a wavelet-based subband decomposition," in *Proc. 1999 Int. Conf. Acoustics, Speech, Signal Processing*, Phoenix, Ariz, USA, March 1999.

[26] T.-C. Hsung, D. P. K. Lun, and W.-C. Siu, "A deblocking technique for block-transform compressed image using wavelet transform modulus maxima," *IEEE Trans. Image Processing*, vol. 7, no. 10, pp. 1488–1496, 1998.

[27] S. Minami and A. Zakhor, "An optimization approach for removing blocking effects in transform coding," *IEEE Trans. Circuits and Systems for Video Technology*, vol. 5, no. 3, pp. 74–82, 1995.

[28] G. Lakhani and N. Zhong, "Derivation of prediction equations for blocking effect reduction," *IEEE Trans. Circuits and Systems for Video Technology*, vol. 9, no. 3, pp. 415–418, 1999.

[29] G. A. Triantafyllidis, D. Tzovaras, and M. G. Strintzis, "Blocking artifact reduction in frequency domain," in *Proc. 2001 IEEE International Conference on Image Processing*, Thessaloniki, Greece, October 2001.

[30] G. A. Triantafyllidis, D. Tzovaras, and M. G. Strintzis, "A novel algorithm for blockiness reduction," in *EURASIP Conference on Digital Signal Processing for Multimedia Communications and Services*, Budapest, Hungary, September 2001.

[31] A. J. Ahumada and R. Horng, "Smoothing DCT compression artifacts," *SID Digest*, vol. 25, pp. 708–711, 1994.

[32] R. L. de Queiroz, "Processing JPEG-compressed images and documents," *IEEE Trans. Image Processing*, vol. 7, no. 12, pp. 1661–1672, 1998.

[33] J. R. Price, "Biased reconstruction for JPEG decoding," *IEEE Signal Processing Letters*, vol. 6, no. 12, pp. 297–299, 1999.

[34] K. R. Rao and P. Yip, *Discrete Cosine Transform: Algorithms, Advantages, Applications*, Academic Press, New York, NY, USA, 1990.

[35] A. Gersho and R. M. Gray, *Vector quantization and signal compression*, Kluwer Academic, Boston, Mass, USA, 1992.

[36] R. C. Reinninger and J. D. Gibson, "Distribution of the two-dimensional DCT coefficients," *IEEE Trans. Communications*, vol. 31, no. 6, pp. 835–839, 1983.

[37] E. Y. Lam and J. W. Goodman, "A mathematical analysis of the DCT coefficient distributions for images," *IEEE Trans. Image Processing*, vol. 9, no. 10, pp. 1661–1666, 2000.

[38] F. Müller, "Distribution shape of two-dimensional DCT coefficients of natural images," *Electronic Letters*, vol. 29, no. 22, pp. 1935–1936, 1993.

[39] K. A. Birney and T. R. Fischer, "On the modeling of DCT and subband image data for compression," *IEEE Trans. Image Processing*, vol. 4, no. 2, pp. 186–193, 1998.

[40] C. L. Nikias and M. Shao, *Signal Processing with Alpha-Stable Distributions and Applications*, John Wiley & Sons, New York, NY, USA, 1995.

[41] T. Lindeberg and J. Garding, "Shape from texture from a multi-scale perspective," in *Proc. 4th International Conference on Computer Vision*, pp. 683–691, Berlin, Germany, May 1993.

[42] W. Forstner and E. Gulch, "A fast operator for detection and precise location of distinct points, corners and centres of circular features," in *Proc. ISPRS Intercommission Workshop*, pp. 281–304, Interlaken, Switzerland, June 1987.

[43] D. Sampson, D. Papadimitriou, and C. Chamzas, "Postprocessing of block-coded images at low bitrates," in *Proc. 1996 IEEE International Conference on Image Processing*, Lausanne, Switzerland, September 1996.

[44] D. Sampson, D. Papadimitriou, M. Ghanbari, and T. Dennis, "A method for enhancing the picture quality for low bit rate block coded images," in *Proc. 1995 IEEE International Conference on Image Processing and Its Applications*, pp. 40–44, Heriot-Watt University, Edinburgh, Scotland, July 1995.

[45] M. Nitzberg and T. Shiota, "Non-linear image filtering with edge and corner enhancement," *IEEE Trans. on Pattern Analysis and Machine Intelligence*, vol. 14, no. 8, pp. 826–833, 1992.

[46] A. C. Bovik and S. Liu, "DCT domain blind measurement of blocking artifacts in DCT-coded images," in *Proc. IEEE Int. Conf. Acoustics, Speech, Signal Processing*, Salt Lake City, Utah, USA, May 2001.

[47] F. X. Coudoux, M. Gzalet, and P. Corlay, "Reduction of blocking effect in DCT-coded images based on a visual perception criterion," *Signal Processing: Image Communication*, vol. 11, no. 3, pp. 179–186, 1998.

[48] S. A. Karunasekera and N. G. Kingsbury, "A distortion measure for blocking artifacts in images based on human visual sensitivity," *IEEE Trans. Image Processing*, vol. 4, no. 6, pp. 713–724, 1995.

George A. Triantafyllidis was born in Thessaloniki, Greece, in 1975. He received the diploma degree from the Electrical Engineering Department of Aristotle University of Thessaloniki, Greece in 1997. He is currently associated with the Information Processing Laboratory of Aristotle University of Thessaloniki, where he is pursuing the Ph.D. degree, and the Informatics and Telematics Institute, Thessaloniki, Greece as a research associate. He has participated in several research projects funded by EU and the Greek Secretariat of research and technology. Since 2000, he serves as a teaching assistant in Aristotle University. His research interests include image compression and analysis as well as monoscopic and stereoscopic image sequence coding and processing.

Dimitrios Tzovaras received the diploma degree in electrical engineering and the Ph.D. degree in 2D and 3D image compression from Aristotle University of Thessaloniki, Thessaloniki, Greece, in 1992 and 1997, respectively. He is a Senior Researcher in the Informatics and Telematics Institute of Thessaloniki. Prior to his current position, he was a Leading Researcher on 3D imaging at the Aristotle University of Thessaloniki. His main research interests include image compression, 3D data processing, virtual reality, medical image communication, 3D motion estimation, and stereo and multiview image sequence coding. His involvement with those research areas has led to the coauthoring of more than 20 papers in refereed journals and more than 50 papers in international conferences. He has served as a regular reviewer for a number of international journals and conferences. Since 1992, he has been involved in more than 20 projects in Greece, funded by the EC, and the Greek Ministry of Research and Technology. Dr. Tzovaras is a member of the Technical Chamber of Greece.

Demetrios Sampson holds a diploma in electrical engineering (1989) from the Department of Electrical Engineering, University of Thrace, Greece, a postgraduate diploma in telecommunication and information systems (1990) and a Ph.D. in electronic systems engineering (1995) from the Department of Electronic Systems Engineering, University of Essex, United Kingdom. He has 12-year professional experience in the design, development, and management of international and national projects in the areas of informatics and telematics. Since 1990, he has participated in thirty-two R&D projects being project leader in twenty of them. He has published more than eighty-five papers in scientific books, journals, and conferences. Dr. Sampson is senior researcher and the head of the Advanced e-Services for the Knowledge Society Research Unit (ASK), at ITI/CERTH and a visiting assistant professor at the University of Peiraias, Greece.

Michael G. Strintzis received the diploma in electrical engineering from the National Technical University of Athens, Athens, Greece in 1967, and the M.S. and Ph.D. degrees in electrical engineering from Princeton University, Princeton, NJ, USA in 1969 and 1970, respectively. He then joined the Electrical Engineering Department at the University of Pittsburgh, Pittsburgh, PA, USA where he served as Assistant (1970–1976) and Associate (1976–1980) Professor. Since 1980 he is professor of electrical and computer engineering at the University of Thessaloniki, and since 1999 Director of the Informatics and Telematics Research Institute in Thessaloniki, Greece. Since 1999 he serves as an Associate Editor of the IEEE Trans. On circuits and systems for video technology. His current research interests include 2D and 3D image coding, image processing, biomedical signal and image processing and DVD and Internet data authentication and copy protection. In 1984, Dr. Strintzis was awarded one of the Centennial Medals of the IEEE.